Research Article Vol. 60, No. 13 / 1 May 2021 / Applied Optics 3801

applied optics

Vibration reconstruction and optical feedback parameter evaluation based on the direction discrimination in self-mixing interferometry

Chol-Yong Ri,[1,*] Jin-Hyok Choe,[1] Hwa-Ryong Ri,[2] Chol-Min Pak,[1] Kyong-Rim Ri,[3] and Jin-Myong O[1]

[1]Faculty of Physics, Kim Il Sung University, Ryongnam-Dong, Taesong District, Pyongyang, Democratic People's Republic of Korea
[2]Faculty of Electronic and Automation, Kim Il Sung University, Ryongnam-Dong, Taesong District, Pyongyang, Democratic People's Republic of Korea
[3]Postgraduate, Kim Il Sung University, Ryongnam-Dong, Taesong District, Pyongyang, Democratic People's Republic of Korea
*Corresponding author: cy.ri1127@ryongnamsan.edu.kp

Received 3 February 2021; revised 23 March 2021; accepted 1 April 2021; posted 2 April 2021 (Doc. ID 421863); published 26 April 2021

Laser diode-based self-mixing interferometry (SMI) is a promising technique for noncontact sensing and its industry. In this paper, a phase unwrapping method in the several optical feedback levels is proposed based on displacement direction. A novel, to the best of our knowledge, method for evaluating the optical feedback factor C simultaneously with the linewidth enhancement is proposed by taking into account the effect of the accuracy of the linewidth enhancement α on the evaluated method for C based on the differential feature of vibration reconstruction signal. Simulations and experiments are conducted to verify the proposed method. © 2021 Optical Society of America

https://doi.org/10.1364/AO.421863

1. INTRODUCTION

Self-mixing interferometry (SMI) has been an active area of research as a powerful technique for noncontact sensing and its instrumentation in recent years [1,2]. In the self-mixing (SM) configuration, laser light is focused onto a remote target, and the light backscattered into the laser cavity is coherently mixed with the lasing field. This phenomenon induces a modulation in frequency and amplitude of the emitted optical field [2,3]. The amplitude modulation can be detected by a monitor photodiode, often included in the laser package; the signal exhibits a periodic modulation, with period equal to half a wavelength. Some applications of the self-mixing interferometry have been demonstrated in different fields of scientific and industrial research [3–9].

Displacement measurement based on the phase unwrapping method (PUM) has advantages. First, it is both convenient and fast; second, it provides high accuracy; and finally, it makes it possible to measure tiny vibrations or displacements. In 1997, Merlo and Donati [10] proposed the first displacement measurement method based on PUM, which achieved the reconstruction accuracy of $\lambda/67$. In 2006, Bes *et al*. [11] improved the aforementioned method by proposing the minimizing operation based on cost function and obtained the optimum predictions of C and α. In 2009, Zabit *et al*. [12] proposed a self-adaptive transition algorithm for fringe detection.

In order to improve the accuracy of the vibration measurement, different methods have been developed [11–15], but all of them are valid for certain ranges of C. The methods proposed in [15–18] can only be applied in the weak feedback regime where $0 < C < 1$, while the method in [11,19] is only valid in the moderate feedback regime where $1 < C < 4.6$. The method in [20] can work in both weak and moderate feedback regimes, but it used a duty cycle algorithm in the weak feedback regime.

The SMI signals depend heavily on the optical feedback factor C. Therefore, there have been proposed a number of methods for estimating C [11,15,16,21,22]. These methods, however, are either limited to a certain feedback level or need a long time for calculation. In [13], a real-time differentiation method has been proposed to evaluate C, but it assumed α is known beforehand.

Since each fringe contributes to the half-wavelength of the laser diode (LD) of displacement amplitude, reconstruction of the target movement from SMI signals relies on the proper extraction of interferometric features from an acquired signal. If fringes are lost during the measurement, the reconstruction will present proportional inaccuracies regardless of the signal processing employed. The standard elaboration of interferometric signal consists in counting the fringes by counting the peaks of the signal derivative with their sign [1,11,20]. This simple elaboration works correctly only in the condition of $1 < C$, when the signal exhibits steep transitions. In this case,

the simple counting of peaks in the signal derivative [1] is no longer applicable for displacement reconstruction. Therefore, there have been proposed an adaptive threshold algorithm [12], fringe detection with the double-derivative algorithm [20], a fringe detection method based on the Hilbert transform [23], and fringe detection through signal analysis [24].

In this paper we present a novel method in applying PUM to any optical feedback level ($0.1 < C$). SMI signal evaluation that is valid for various optical feedback levels is very useful in implementing a low-cost embedded SMI sensor without requiring any additional devices or algorithms [20]. We also present an evaluation method for both the optical feedback factor C and the linewidth enhancement factor α by taking into account the effect of the linewidth enhancement on evaluation for C based on differential feature of vibration reconstruction signal [13]. This method allows us to evaluate both C and α at various optical feedback levels. So it offers the possibility to reconstruct the vibration in different optical feedback levels and evaluate the parameters of SMI signals. The proposed method is verified by using simulations and experiments for various waveforms.

2. PHASE UNWRAPPING

The basic theoretical model for an SMI system is given by [15]

$$p(t) = p_0\{1 + m \cdot g(t)\}, \tag{1}$$

$$g(t) = \cos(x_F(t)), \tag{2}$$

$$x_0(t) = x_F(t) + C \cdot \sin[x_F(t) + \arctan(\alpha)], \tag{3}$$

$$x_0(n) = 4\pi L(t)/\lambda_0, \tag{4}$$

where p_0 is the power emitted by the LD in a free running state, m is a modulation index, x_F is the interferometric phase subject to back-reflections, x_0 is the original phase, $L(t)$ is the distance between the LD facet and the external target, C and α are the optical feedback factor and LD's linewidth enhancement factor, respectively. Note that $g(t)$ can be derived from $p(t)$ using Eq. (1) and $L(t)$ from $x_0(t)$ using Eq. (4). Therefore, the keys to signal processing are to estimate $x_F(t)$ from $g(t)$ and then to estimate $x_0(t)$ from $x_F(t)$.

A rough estimation of x_F can be done by normalizing the optical output power (OOP) from Eq. (1), such as $P_N = p(t)/p_0$, and applying the inverse cosine function, i.e.,

$$\hat{x}_f(t) = \arccos[P_N(t)]. \tag{5}$$

Next, fringe detection is performed. Based on the detection result, the phase when optical feedback exists, $x_F(t)$, can be estimated by adding 2π to or subtracting 2π from $\hat{x}_f(t)$. At this step, unlike the previous implementations, it is proposed to perform estimation of $\hat{x}_f(t)$ not based on the result of fringe detection but based on the information of displacement direction.

Considering the generation condition of SMI signal [25], when one point $x_F(n)$ is known for the phase signal $x_F(t)$, its neighboring point $x_F(n+1)$ can take one of the following values:

$$x_{F,1}(n+1) = \arccos[P_N(n+1)] + 2k_1\pi,$$
$$x_{F,2}(n+1) = -\arccos[P_N(n+1)] + 2k_2\pi, \tag{6}$$

where k_1, k_2 are integers as in [20] and can be expressed as the following equations when the displacement is in the increasing direction (DIR $= +1$):

$$k_1 = \text{ceil}\left[\frac{\pi}{2}(x_F(n) - \arccos[P_N(n+1)])\right],$$
$$k_2 = \text{ceil}\left[\frac{\pi}{2}(x_F(n) + \arccos[P_N(n+1)])\right]. \tag{7}$$

Similarly, when the displacement is in the decreasing direction, (DIR $= -1$) k_1, k_2 can be expressed as

$$k_1 = \text{floor}\left[\frac{\pi}{2}(x_F(n) - \arccos[P_N(n+1)])\right],$$
$$k_2 = \text{floor}\left[\frac{\pi}{2}(x_F(n) + \arccos[P_N(n+1)])\right]. \tag{8}$$

When the optical feedback factor is $C > 1$, the two neighboring points of $x_F(t)$ may be considered either continuous or discontinuous. When the distance between these two points is close enough to be considered continuous, between $x_{F,1}(n+1)$ and $x_{F,2}(n+1)$, the one with the shorter distance from $x_F(n)$ has the larger probability to be $x_F(n+1)$. On the contrary, when these two points are discontinuous, the one with the larger distance from $x_F(n)$ has the larger probability to be $x_F(n+1)$. Therefore, both $x_{F,1}(n+1)$ and $x_{F,2}(n+1)$ have nonzero probabilities to be $x_F(n+1)$.

We now investigate which value will be actually realized. From Eq. (1), we obtain the following relationship among three neighboring values of the normalized SMI signal $P_N(t)$ and the phase signal $x_F(t)$:

$$\frac{P_N(n+1) - P_N(n)}{P_N(n) - P_N(n-1)} = \frac{\cos(x_F(n+1)) - \cos(x_F(n))}{\cos(x_F(n)) - \cos(x_F(n-1))}. \tag{9}$$

Therefore, using Eq. (9), $x_F(n+1)$ can be determined from its previous two values, that is, Eq. (9) can be used to select one between $x_{F,1}(n+1)$ and $x_{F,2}(n+1)$, which are determined from Eqs. (6)–(8). When $x_{F,1}(n+1)$ and $x_{F,2}(n+1)$ are very close to each other, $x_F(n+1)$ determined in this way might be different from the actual value (Fig. 2).

Now, the following processes can be used to confirm and to correct the value of $x_F(n)$. Similarly to the case of $x_F(n+1)$, when one point $x_F(n)$ is known for the phase signal $x_F(t)$, its neighboring point $x_F(n-1)$ can take one of the following values:

$$x_{F,1}(n-1) = \arccos[P_N(n-1)] + 2k_1\pi,$$
$$x_{F,2}(n-1) = -\arccos[P_N(n-1)] + 2k_2\pi. \tag{10}$$

If DIR $= +1$,

$$k_1 = \text{floor}\left[\frac{\pi}{2}(x_F(n) - \arccos[P_N(n-1)])\right],$$
$$k_2 = \text{floor}\left[\frac{\pi}{2}\left(x_F(n) + \arccos[P_N(n-1)]\right)\right], \tag{11}$$

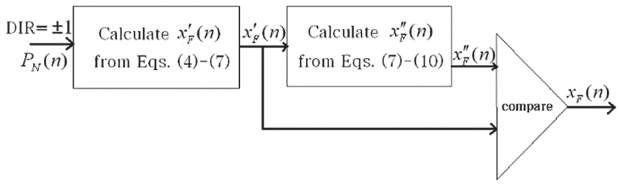

Fig. 1. Phase (x_F) evaluation algorithm for SMI based on the information of displacement direction.

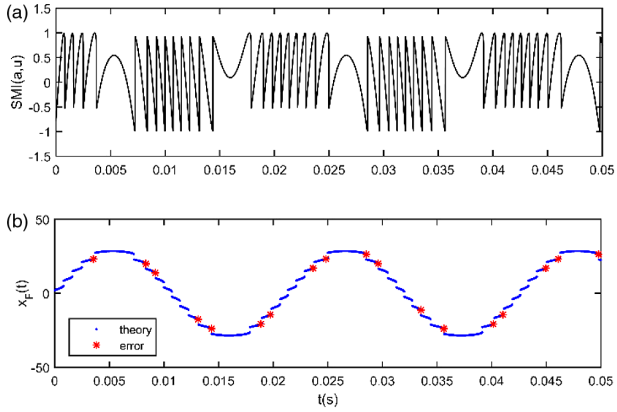

Fig. 2. Comparison between the theoretical values and the calculated values using the algorithm in Fig. 1. (a) SMI wave; (b) rough estimation of phase $x_F(t)$.

and if DIR $= -1$,

$$k_1 = \text{ceil}\left[\frac{\pi}{2}\left(x_F(n) - \arccos[P_N(n-1)]\right)\right],$$

$$k_2 = \text{ceil}\left[\frac{\pi}{2}\left(x_F(n) + \arccos[P_N(n-1)]\right)\right]. \quad \textbf{(12)}$$

Phase signals $x'_F(n)$ can be obtained from Eqs. (6)–(9), which can in turn be used to calculate $x''_F(n)$ from Eqs. (9)–(12). Then only those elements that share the same value in both $x'_F(n)$ and $x''_F(n)$ are selected to be $x_F(n)$ (Fig. 1). Values obtained in this way coincide with the actual phase signals. Different values of $x'_F(n)$ and $x''_F(n)$ correspond to the cases when the values of $x_{F,1}(n)$ and $x_{F,2}(n)$ are very close to each other, which happen relatively rarely, so it is safe to omit these cases in data process.

Figure 2 shows the differences between the actual values and the values calculated using the proposed algorithm in Fig. 1. As the proposed algorithm can be used to detect the difference points shown in Fig. 2(b), these points are omitted in data processing.

Using the proposed algorithm, phase signals for SMI can be calculated precisely based on the accurate direction information without the need for fringe detection. The major advantage of this approach is that even when fringe detection fails for some portion of data, it is possible to reconstruct the displacement precisely based on the accurate information on displacement direction, and, even in the weak feedback regime where fringe detection does not work well, phase unwrapping may still be possible.

3. ESTIMATION OF C AND α

In the next stage of PUM, the optical feedback factor C and the linewidth enhancement factor α are estimated so as to evaluate the initial phase of displacement $x_0(t)$. In [13], it was proposed to estimate the optical feedback factor C in real time by using differential characteristics of reconstructed signal. However, this method is applicable when the linewidth enhancement α is known beforehand, and in this case the evaluated value of C differs from its real one. That is, the evaluated value of C depends on the accuracy of the linewidth enhancement α. So both the optical feedback factor and the linewidth enhancement are estimated simultaneously using the effect of the linewidth enhancement α on the evaluation for C.

As shown in Fig. 7 in Ref. [13], when α is known, the amplitude of differential signal of reconstructed displacement with C has the minimum value (at zero) near the actual value of C. In this case the amplitude of differential signal increases in linear proportion to C [Fig. 3(a)]. Similarly, when C is known, the amplitude of differential signal increase monotonically, not linearly with α [Fig. 3(b)]. In both cases the directions of amplitude of differential signal differ from each other, and the amplitude for C is larger than for α (Fig. 4). That is, the effect of α on C is stronger than that of C on α. So, similarly to [13,26], the optical parameters are estimated simultaneously by iterated evaluation for both C and α, but this is possible for $C > 1.5$ because the effect of α is stronger with decreasing C.

When α is known, the amplitude of reconstruction differential signal does not increase linearly with α near the zero point (Fig. 5). That is, the differential signal no longer has the linear feature. Because when C and α approach their actual values near the zero point, the amplitudes of differential signal are very similar to each other, and when both C and α change, the differential signals for both cases in Fig. 4 are mixed.

Near the zero point in Fig. 5, either the reentering phenomenon for $\alpha_x < \alpha_0$ or the convex one for $\alpha_x > \alpha_0$ occurs dominantly. So C and α may be estimated by using the halving method to minimize the shape of either the reentering or convex. For $C_0 > 1.5$, either the reentering or convex shape occurs with α_x like in Fig. 5, but for $C_0 < 1.5$ this does not occur correctly (Fig. 6). But we can find the difference between two

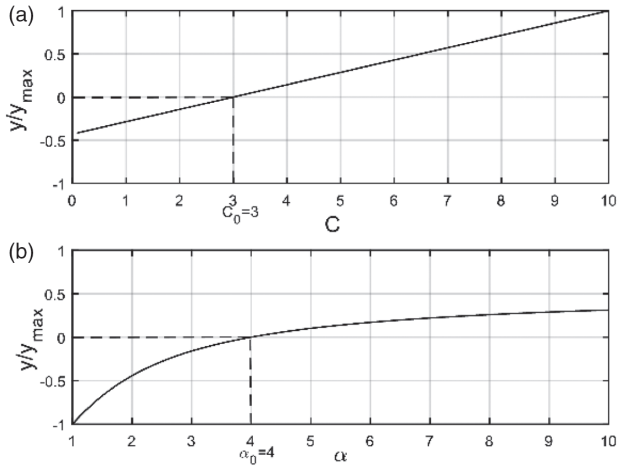

Fig. 3. Monotonic increase of amplitude of displacement reconstruction differential signal for $C_0 = 3$, $\alpha_0 = 4$. (a) $\alpha_0 = 4$; (b) $C_0 = 3$.

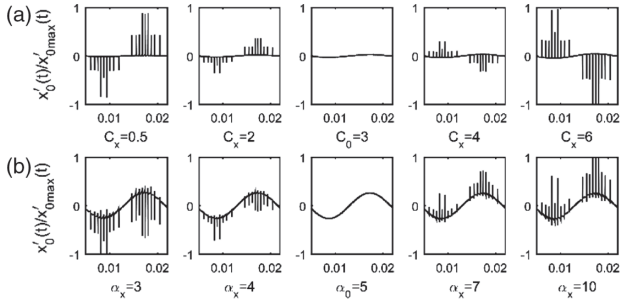

Fig. 4. Displacement reconstruction differential signal (a) for known α and (b) for known C.

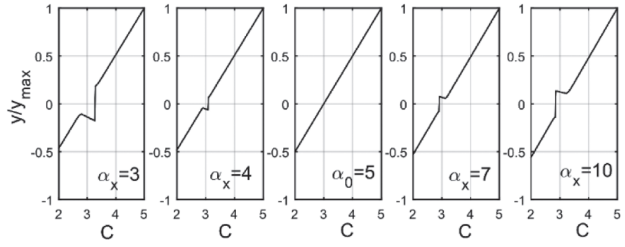

Fig. 5. Amplitude of displacement reconstruction differential signal according to C and α.

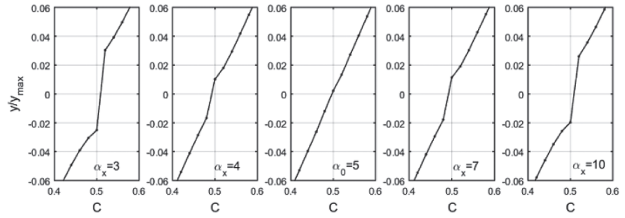

Fig. 6. Amplitude of differential signal near zero cross point for $C < 1.5$.

amplitudes of differential signal near the zero point; d is minimized as α_x approaches α_0. So, for $C_0 < 1.5$, α is determined by estimating the point with minimal difference of two amplitudes of differential signal near the zero point.

Therefore, the following procedure can be used to evaluate C and α.

(1) In the displacement reconstruction signal, $C_{\max}$ and $C_{\min}$ are evaluated from $\alpha_{\min}$ and $\alpha_{\max}$, respectively, in the range $[C_1, C_2]$ by using step 3), and $[C_{\min}, C_{\max}]$ is set to the range for evaluating C, where the range $[C_1, C_2]$ is the initial range for evaluating of C, for example, $[0.1, 20]$. $\alpha_{\min}$ and $\alpha_{\max}$ are also found in the same way. Evaluated $C_{\min}$ and $C_{\max}$ are the minimum and maximum of C where the reentering or convex shape may occur near the zero point. So computational cost for the latter step can decrease.

(2) In the range $[C_{\min}, C_{\max}]$, α is fixed, and the amplitude difference of the differential signal d is evaluated by using the halving method.

(3) In the range $[\alpha_{\min}, \alpha_{\max}]$, when either d is minimum (for $C_{\min} < 1.5$) or d is zero (for $C_{\min} > 1.5$), α_0 is evaluated by using either the range dividing method or the halving method. In this step, d corresponding to each value for α is evaluated by using the step 2).

(4) In the case of α_0, C_0 for $d \approx 0$ is evaluated by using the halving method in the range $[C_{\min}, C_{\max}]$.

In the above procedure, the halving method can reduce the computational cost. The proposed method obtains the curve for the amplitude difference (d) of the differential signal in the range $[C_{\min}, C_{\max}]$ and finds α near the zero point to determine α_0. Then C_0 is determined similar to [13] by using α_0. So this algorithm has the advantage that both the optical feedback factor C and the linewidth enhancement α can be evaluated in various feedback regimes, especially in the weak feedback regime.

4. ESTIMATION OF DISPLACEMENT DIRECTION

PUM based on fringe detection is difficult to apply to $C < 1$ due to fringe fading. Because detection of displacement direction is vital to the aforementioned algorithms, another algorithm is developed to detect displacement direction based on a simple derivative method combined with special treatment (Fig. 7).

In conventional methods for fringe detection [11,12], values obtained via an *arcos* function from normalized input signals are differential and processed. This type of processing is not appropriate in the weak feedback regime because it makes not only fringe peaks but also their opposite peaks prominent [Fig. 8(a)]. We propose to use signals that are products of normalized SMI derivative $P_N(t)$ and conventional derivative for fringe detection (Fig. 7). Note that when multiplying two derivative values at each moment, their signs should be considered carefully. Doing so makes only the fringe peaks prominent. As a result, drawbacks of the simple derivative method are successfully overcome, and fringe points along the displacement direction are made outstanding for $1 > C$ [Fig. 8(b)].

When fringe detection methods such as the adaptive transition detection algorithm [12] are applied to this signal, information on fringe points can be obtained. As the peaks in the two aforementioned derivative signals approach maximum/minimum (convex/concave) near the fringe points (not applicable elsewhere), the proposed algorithm in Fig. 7 makes only the fringe peaks prominent [Figs. 8(a) and 8(b)]. In addition, detection of local maxima and minima is performed with a moving average window over five intervals [Fig. 8(c)]. This adds a noise-resistant feature to the proposed algorithm.

Finally, displacement direction is determined from the locations and signs of local maxima and minima. Note that these local maxima and minima may or may not coincide with traditional fringe points. Even if fringe fading occurs due to weak

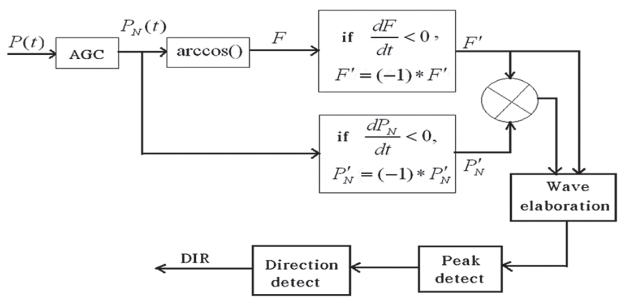

Fig. 7. Algorithm to detect displacement direction.

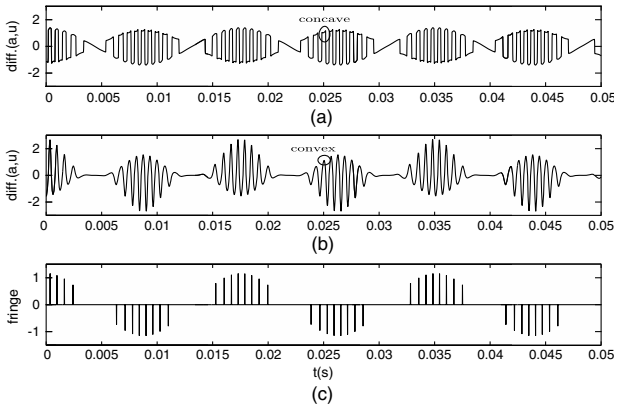

Fig. 8. Fringe detection comparison when $C = 1$ and $\alpha = 3.04$. (a) Conventional method, (b) proposed method, (c) fringe detection result with the proposed method.

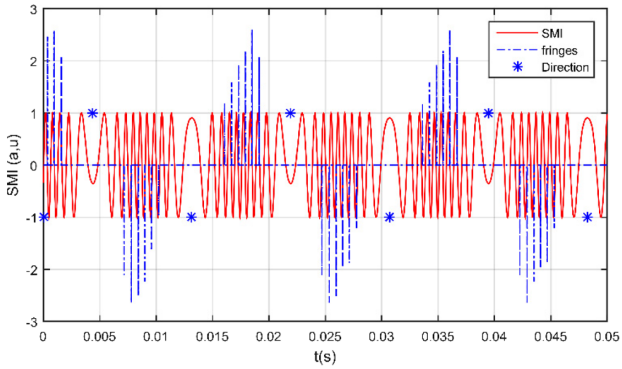

Fig. 9. Fringe detection result.

feedback condition and noise, it is still possible to determine displacement direction (Fig. 9).

5. VERIFICATION

A. Simulation

1. Verification on $x_F(n)$

In order to verify the proposed algorithm, we use the simulation data generated by the SMI model described in [25] and apply the proposed algorithm to the data. We assume that the external target vibrates in a sinusoidal form. Therefore, its corresponding $x_0(t)$ has a peak-to-peak amplitude of 1.5 μm and fundamental frequency of 57 Hz. We assume the LD's wavelength is 650 nm.

In order to verify the effect of the fringe fading on the vibration reconstruction, in our simulation we assume $C = 0.04$ and $\alpha = 3.04$. The simulation result is illustrated in Fig. 9. Figure 9 shows fringe fading for $C = 0.04$. Figure 10, however, shows that direction evaluation and displacement reconstruction are performed accurately. These results suggest that the proposed method is not dependent on fringe detection result and that reconstruction can be performed solely based on displacement direction, and that even in noisy environment accurate reconstruction is still possible whether fringe detection is successful or not.

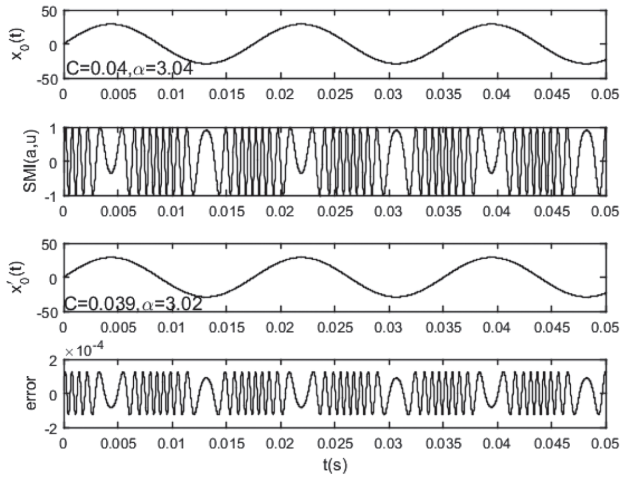

Fig. 10. Reconstruction result in the weak feedback regime.

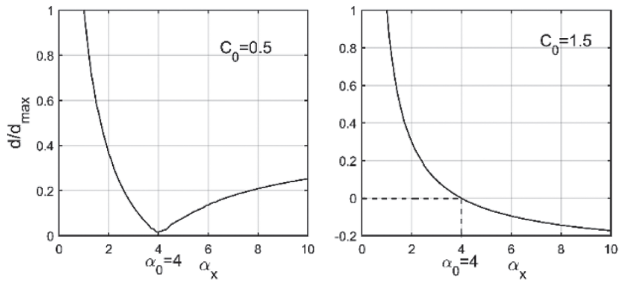

Fig. 11. Plot of d obtained from SMI signal [(a) for $C_0 = 0.5$, $\alpha_0 = 4$; (b) for $C_0 = 1.5, \alpha_0 = 4$].

2. Verification for Evaluating C and α

Simulation conditions are the same as in the previous case, and the target vibration is assumed to be sinusoidal. Figure 11 plots the difference of amplitude of differential signal obtained from SMI for (a) $C_0 = 0.5$, $\alpha_0 = 4$ and $C_0 = 1.5$, $\alpha_0 = 4$. In Fig. 11(a), d is the difference of amplitude of differential signal, without taking into account the direction of reentering and convex shape of SMI signal, while their directions are taken into account in Fig. 11(b), where reentering and convex shapes are denoted by "+" and "−", respectively. This figure shows that d is either minimum or zero for $\alpha_0 = 4$. The method used in Fig. 11(a) is applicable in the whole range of C, but the evaluation time takes longer than the method for Fig. 11(b). Thus it is better to use only for $C < 1.5$.

Tables 1 and 2 show the estimation results for SMI signals for various C and $\alpha = 3.7$ and various α and $C = 3.2$. [$C_{\max}$, $C_{\min}$] and [$\alpha_{\max}$, $\alpha_{\min}$] are taken as [0.1, 20] and [1,20], respectively. Table 1 illustrates that the proposed method can be used to estimate C and α with relatively higher accuracies. It also illustrates that the error in C rarely depends on the error in α because by using this method α is first evaluated and then C is evaluated, and α rarely affects the C estimation. Table 2 illustrates that as α increases the error in α also increases a small amount; however, estimated α is relatively accurate. It is a reason why the error increases, because the slope for the difference curve of the amplitude of differential signals gets flat near the zero point as α increases.

Table 1. Evaluation Results for C and α when α is Fixed

No.	True C	True α	Estimated C	Estimated α	C error
1	0.2	3.7	0.198	3.77	0.002
2	0.3	3.7	0.299	3.71	0.001
3	0.5	3.7	0.4995	3.7	0.0005
4	0.8	3.7	0.7997	3.77	0.0003
5	1	3.7	0.9998	3.7	0.0002
6	2	3.7	1.9996	3.69	0.0004
7	3	3.7	2.9997	3.7	0.0003
8	4	3.7	3.9996	3.7	0.0004
9	6	3.7	5.9994	3.7	0.0006

Table 2. Evaluation Results for C and α when C is Fixed

No.	True C	True α	Estimated C	Estimated α	α error
1	3.2	3	3.1997	3.000	0
2	3.2	4	3.1993	3.99	0.01
3	3.2	5.6	3.1995	5.59	0.01
4	3.2	8.9	3.1995	8.87	0.03
5	3.2	12.9	3.1997	12.86	0.04

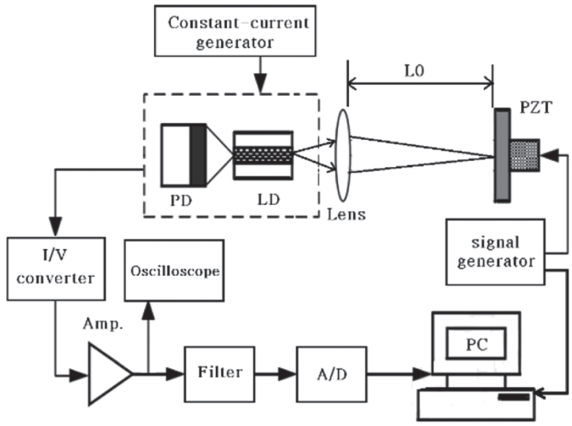

Fig. 12. Experimental SMI configuration.

B. Experiment

Experiments are also conducted to verify the effectiveness of the proposed method using the measurement data in [26]. A low-cost LD (QL65D5SA, QSI) with center wavelength 650 nm is employed in experiments (Fig. 12). In the experiment, the LD is controlled by a rectified current source without any temperature control. Output power and current are set at 5 mW and 28 mA, respectively. A piezoelectric ceramic vibrator is used to form the external cavity with the initial cavity length of 50 mm (L0).

The experimental data are filtered in the same way as in [26]. Using the signal treatment method suggested in [20], filtered signal is then treated by setting the scale factor as the average of discontinuities in each direction.

The phase unwrapping of the normalized SMI waveform is performed to obtain the interfered phase $x_F(t)$ by using the proposed method [Fig. 14(b)]. C and α are evaluated with $x_F(t)$

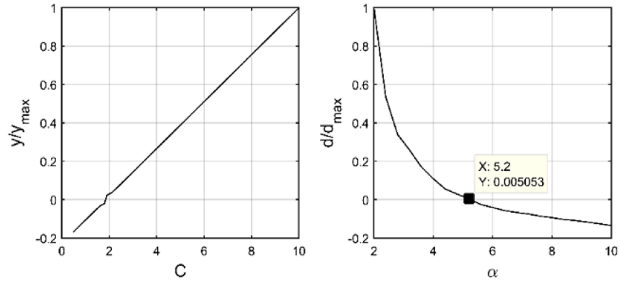

Fig. 13. Plot of differential features of displacement reconstruction obtained from experimental SMI signal. (a) C versus amplitude of differential signal; (b) α versus difference of amplitude of differential signal.

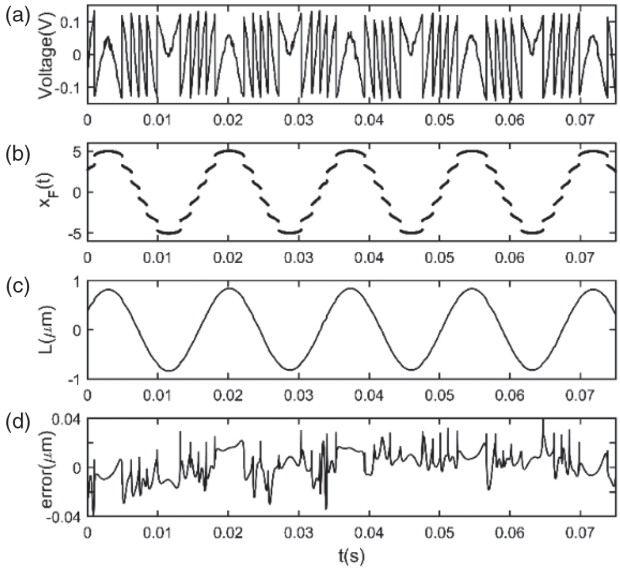

Fig. 14. Reconstruction result from experimental SMI signal. (a) Experimental SMI waveform, (b) optical feedback phase $x_F(t)$, (c) reconstructed displacement, (d) residual error between real and reconstructed displacements.

using the proposed method for estimating the optical parameters. The estimation results are $\alpha = 5.214$ and $C = 1.848$. Figure 13 illustrates the plot for C versus the amplitude of differential signal of reconstructed displacement and α versus the difference of amplitude of the differential signal.

In Fig. 14(a), the reentering and convex shape appear near the zero point because there is some noise in the measured data, unlike in the simulation.

Finally, the initial phase $x_F(t)$ is evaluated from $x_F(t)$, as well as C and α obtained from the proposed method, and reconstructed displacement is obtained from it (Fig. 14). The result for the amplitude of vibration is 1.656 μm (the amplitude is V_{pp}). The result obtained from the proposed method is similar to [26], and the proposed method can be applied to SMI (Table 3)

Most SMI experiments so far employed either distributed feedback lasers or Fabry–Perot lasers at near-infrared wavelength as their LDs [20,21,23]. The proposed method may produce better results when different LDs, semiconductor laser driver units, and temperature controller units are used. In

Table 3. Estimation for C and α from Experimental SMI

Parameter	Method in [26]	Proposed Method
C	1.770	1.848
α	5.686	5.214
f_0 (Hz)	58.0	58.07
L_0 (μm)	1.658	1.656

addition, this work may contribute to implementing SMIs with low-power, cost-effective semiconductor LDs, which makes it possible to build low-cost SMIs to provide convenient collimation and to simplify the safety precautions for instrument operation.

6. CONCLUSIONS

In this paper we developed a vibration reconstruction method based on the direction discrimination in SMI of various optical feedback levels. A PUM has been proposed that depends on displacement direction, not on fringe detection, and an estimation algorithm has been suggested for evaluating the optical feedback factor and the linewidth enhancement factor, all of which have been verified through simulations and experiments for various optical feedback levels ($0.1 < C$) of SMI to produce good agreements, even when fringe detection fails in the weak feedback regime. Our work also provides the algorithm for evaluating C and α by considering the effect of the linewidth enhancement on linear increase feature of amplitude of differential signal of reconstruction signal.

Unlike the conventional reconstruction methods that are susceptible to fringe fading due to noise and weak feedback levels, the proposed method can be applied for reconstructing vibrations in a wider feedback range with an improved noise immunity, which makes it possible to simplify SMI configurations and to lower instrument costs.

The method proposed in this paper is valid in various feedback regimes ($C > 0.1$) with partial applications in estimating feedback factor and linewidth enhancement factor and in detecting fringe points.

Funding. National Program on Key Science Research of DPR Korea (9-3-2).

Disclosures. The authors declare no conflicts of interest.

Data Availability. Data underlying the results presented in this paper are not publicly available at this time but may be obtained from the authors upon reasonable request.

REFERENCES

1. G. Giuliani, M. Norgia, S. Donati, and T. Bosch, "Laser diode self-mixing technique for sensing applications," J. Opt. A **4**, S283–S294 (2002).
2. T. Bosch, N. Servagent, and S. Donati, "Optical feedback interferometry for sensing application," Opt. Eng. **40**, 20–27 (2001).
3. M. T. Fathi and S. Donati, "Thickness measurement of transparent plates by a self-mixing interferometer," Opt. Lett. **35**, 1844–1846 (2010).
4. D. Han, S. He, L. Fan, L. Ma, and H. Wang, "Real time velocity measurement with speckle modulation of a Q-resonator," Opt. Laser Technol. **47**, 76–79 (2013).
5. R. Luigi, C. Stefano, and P. Nithiyanantham, "Measurement of the fluid-velocity profile using a self-mixing super luminescent diode," Meas. Sci. Technol. **22**, 025402 (2011).
6. M. Norgia, G. Giuliani, and S. Donati, "Absolute distance measurement with improved accuracy using laser diode self-mixing interferometry in a closed loop," IEEE Trans. Instrum. Meas. **56**, 1894–1900 (2007).
7. W. Chen, S. Zhang, and X. Long, "Angle measurement with laser feedback instrument," Opt. Express **21**, 8044–8050 (2013).
8. S. Shinohara, A. Mochizuki, H. Yoshida, and M. Sumi, "Laser Doppler velocimetry using the self-mixing effect of a semiconductor laser diode," Appl. Opt. **25**, 1417–1419 (1986).
9. S. Donati, "Developing self-mixing interferometry for instrumentation and measurements," Laser Photon. Rev. **6**, 393–417 (2012).
10. S. Merlo and S. Donati, "Reconstruction of displacement waveforms with a single-channel laser-diode feedback interferometer," IEEE J. Quantum Electron. **33**, 527–531 (1997).
11. C. Bes, G. Plantier, and T. Bosch, "Displacement measurements using a self-mixing laser diode under moderate feedback," IEEE Trans. Instrum. Meas. **55**, 1101–1105 (2006).
12. U. Zabit, T. Bosch, and F. Bony, "Adaptive transition detection algorithm for a self-mixing displacement sensor," IEEE Sens. J. **9**, 1879–1886 (2009).
13. Y. Fan, Y. Yu, J. Xi, and J. Chicharo, "Improving the measurement performance for a self-mixing interferometry-based displacement sensing system," Appl. Opt. **50**, 5064–5072 (2011).
14. O. D. Bernal, U. Zabit, and T. Bosch, "Study of laser feedback phase under self-mixing leading to improved phase unwrapping for vibration sensing," IEEE Sens. J. **13**, 4962–4971 (2013).
15. Y. Yu, J. Xi, J. Chicharo, and T. Bosch, "Toward automatic measurement of the linewidth-enhancement factor using optical feedback self-mixing interferometry with weak optical feedback," IEEE J. Quantum Electron. **43**, 527–534 (2007).
16. W. Lu, J. Xi, Y. Yu, and J. Chicharo, "Linewidth enhancement factor measurement based on optical feedback self-mixing effect: a genetic algorithm approach," J. Opt. A **11**, 045401 (2009).
17. J. Xi, Y. Yu, J. Chicharo, and T. Bosch, "Estimating the parameters of semiconductor lasers based on weak optical feedback self-mixing interferometry," IEEE J. Quantum Electron. **41**, 1058–1064 (2005).
18. N. Servagent, F. Gouaux, and T. Bosch, "Measurements of displacement using the self-mixing interference in a laser diode," J. Opt. **29**, 168–173 (1998).
19. G. Giuliani, S. Bozzi-Pietra, and S. Donati, "Self-mixing laser diode vibrometer," Meas. Sci. Technol. **14**, 24–32 (2003).
20. A. Magnani, A. Pesatori, and M. Norgia, "Self-mixing vibrometer with real-time digital signal elaboration," Appl. Opt. **51**, 5318–5325 (2012).
21. K. Cholhyon, L. Cholman, and O. Kwonhyok, "Effect of linewitdth enhancement factor on fringe in a self-mixing signal and improved estimation of feedback factor in laser diode," IEEE Access **7**, 28886–28893 (2018).
22. Y. Yu, G. Giuliani, and S. Donati, "Measurement of the linewidth enhancement factor of semiconductor lasers based on the optical feedback self-mixing effect," IEEE Photon. Technol. Lett. **16**, 990–992 (2004).
23. A. L. Arriaga, F. Bony, and T. Bosch, "Speckle-insensitive fringe detection method based on Hilbert transform for self-mixing interferometry," Appl. Opt. **53**, 6954–6962 (2014).
24. A. L. Arriaga, F. Bony, and T. Bosch, "Real-time algorithm for versatile displacement sensors based on self-mixing interferometry," IEEE Sens. J. **16**, 195–202 (2016).
25. R. Kliese, T. Taimre, A. Ashrif, A. Bakar, Y. L. Lim, K. Bertling, M. Nikolić, J. Perchoux, T. Bosch, and A. D. Rakić, "Solving self-mixing equations for arbitrary feedback levels: a concise algorithm," Appl. Opt. **53**, 3723–3736 (2014).
26. C.-Y. Ri, C.-S. Kim, G.-C. Ri, J.-C. Kang, C.-M. Pak, and J.-M. O, "Evaluation method for the optical feedback factor and linewidth enhancement factor using phase discontinuities in self-mixing interferometry signals," Appl. Opt. **59**, 687–693 (2020).